CHAPTER 6: DATA INTEGRATION OF REMOTE SENSED AND GROUND PENETRATING RADAR SURVEY DATA

The data from the LiDAR surveys has been combined with the GPR data in two ways. Firstly, the LiDAR data has been used for the presentation and analysis of the GPR results (chapter 5) and was layered with the GPR data in ArcGIS. In addition specific GPR surveys have been integrated with the LiDAR data and layered in a quasi 3D environment using ArcScene.

Combining these two data sources has importance for several reasons. Both methods provide a means of cross validating the results obtained through the other, and in nearly all cases the correlation between the LiDAR and the GPR data has been good. The combination of the two techniques also allows a 2D plot produced by LiDAR to have the third stratigraphic element added through GPR. Lastly, it is important to develop methods of integrating remote sensed and ground prospection based methods, as both are set to play an increasing role in geoarchaeological investigations.

6.1 Integration in ArcScene

Four GPR surveys were combined with LiDAR data, being surveys MFG1, T1G1, T1G3 and T2G1. For each survey it was not possible to show all the depth slice data, so specific depth slices have been selected.

6.1.1 Integration of MFG1 and LiDAR data

The integration of MFG1 with the LiDAR data used the LiDAR last pulse DTM, combined with the depth slices of 1.4m – 1.6m and 2.4m - 2.6m (Fig. 6.1). From this image the correlation between the LiDAR DTM and the GPR depth slice stratigraphy is particularly powerful. The palaeochannels MFC1, MFC2 and MFC3 are visible in the LiDAR and in the GPR depth slices as are the gravel deposits MF3 and MF4. This image demonstrates how sub surface stratigraphy can be imaged in the surface topography.

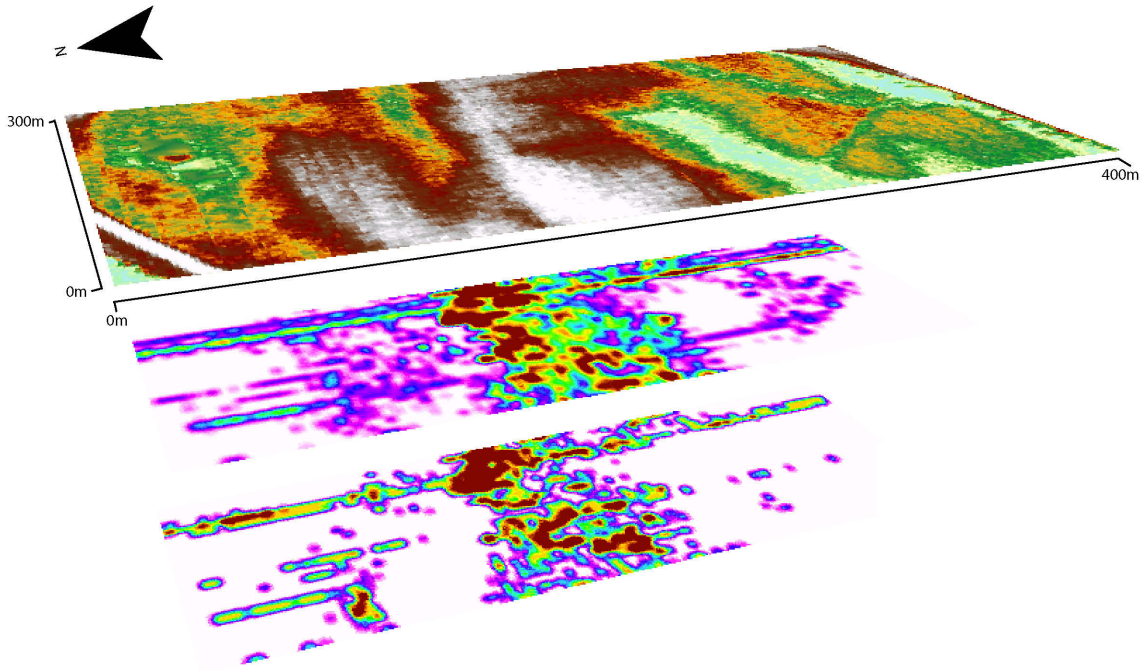

Fig 6.1: The LiDAR last pulse DTM combined with the 1.4m – 1.6m and 2.4m – 2.6m depth slices on the MFG1 survey.

6.1.2 Integration of T1G1 and LiDAR

The integration of the T1G1 survey used the LiDAR intensity plot combined with the GPR depth slices of 0.4m – 0.6m, 0.9m - 1.1m, 1.9m – 2.1m and 2.4m – 2.6m (Fig. 6.2). The correlation between the LiDAR intensity and the GPR depth slices is excellent. Terrace 1 is visible in the LiDAR intensity and also in the GPR depth slices, as is the palaeochannel T1C6. With movement down through the GPR depth slices the same features are evident but the reflectance values change. For example at 0.4m – 0.6m terrace 1 is a higher reflecting unit than the palaeochannel, although this is depth slicing in alluvium on top of the terrace gravels. Below this at 0.9m – 1.1m the palaeochannel T1C6 is shown as a higher reflecting unit than terrace1, although at this depth the terrace 1 gravel are still buried under alluvium. At the 1.9m – 2.1m this reflectance has changed again, with the terrace 1 gravels being clearly evident, as at 2.4m – 2.6m. The difference in the GPR reflectance between the terrace 1 and the palaeochannel is a product of different sediment types. It would appear that the LiDAR intensity values map these different sediments through changes in the sediment water content. As suggested in chapter 4, LiDAR intensity appears to have the ability to map changes in sediment structure through soil moisture content. These changes are confirmed through the GPR depth slices.

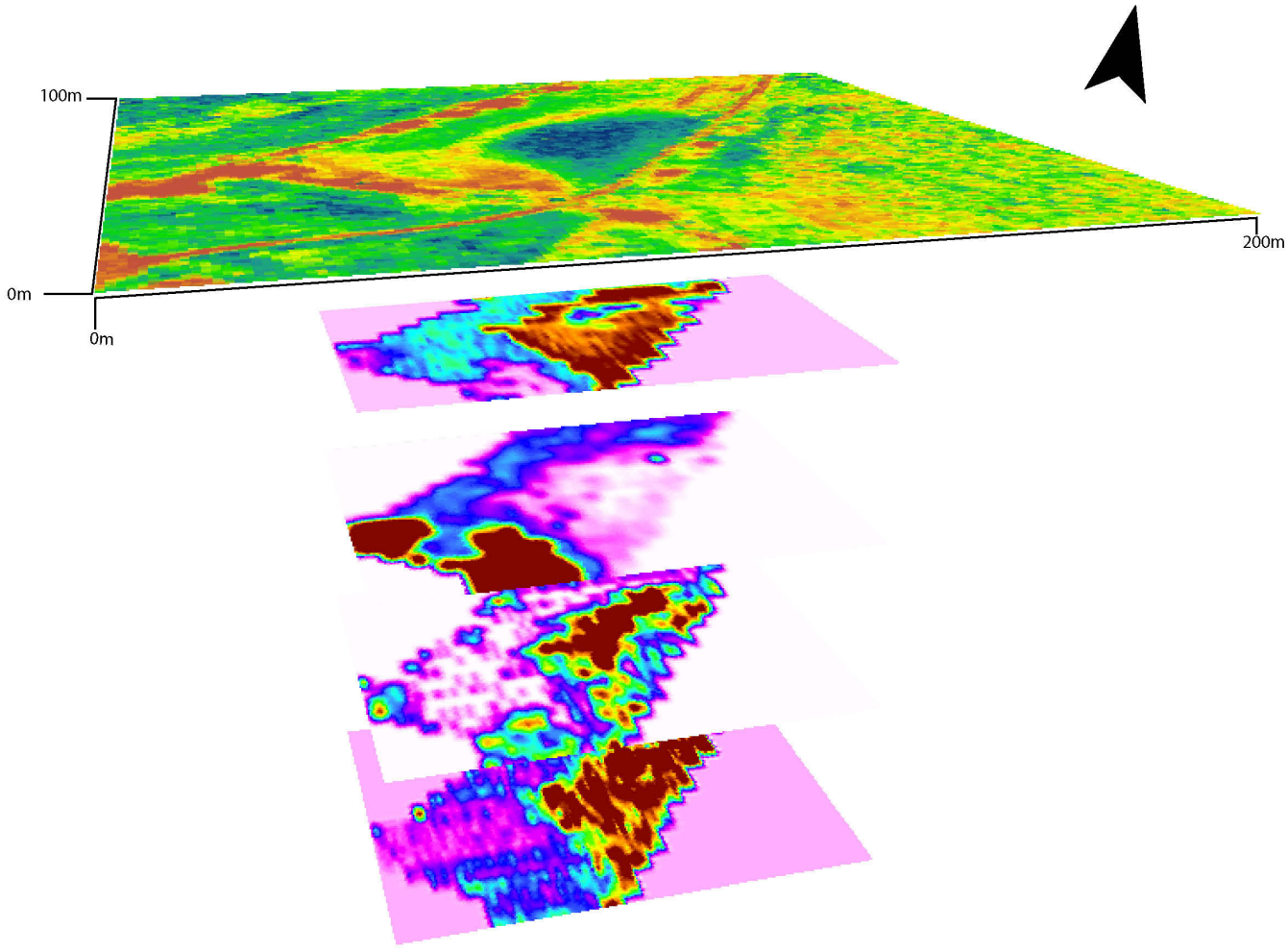

Fig 6.2: The T1G1 survey combing the GPR depth slices of 0.4m – 0.6m, 0.9m - 1.1m, 1.9m – 2.1m and 2.4m – 2.6m with the LiDAR intensity.

6.1.3 Integration of T1G3 and LiDAR

The T1G3 also investigated an area of terrace 1 with associated palaeochannel. The integration used the LiDAR last pulse DTM combined with the GPR 0.4m – 0.6m, 1.4m – 1.6m and 2.4m – 2.6m depth slices (Fig. 6.3). The relationship between the topography identified by the LiDAR and the GPR depth slices is excellent. The palaeochannel T1C8 is clearly visible in the LiDAR DTM and in the 0.4m – 0.6m and 1.4m –1.6m depth slices. Again with movement down through the depth slices the reflectance values change, for example at 0.4m – 0.6m terrace 1 is shown as a high reflecting unit. At 1.4m – 1.6m the palaeochannel T1C8 is the highest reflecting unit. By the 2.4m – 2.6m the limit of effective penetration has been reached, although some higher reflecting gravels are visible on terrace 1.

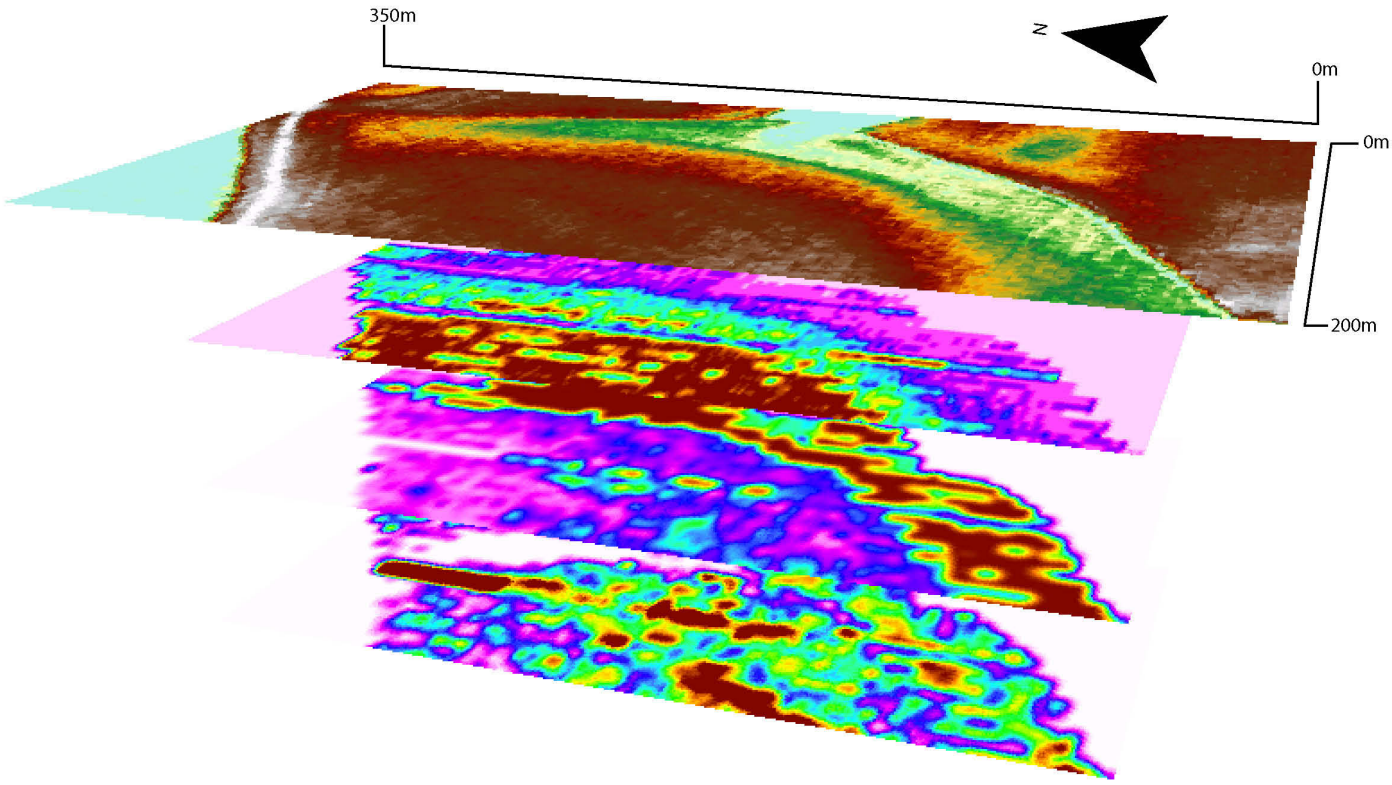

Fig 6.3: The T1G3 survey combining the GPR depth slices of 0.4m – 0.6m, 1.4m – 1.6m and 2.4m – 2.6m with the LiDAR last pulse DTM.

6.1.4 Integration of T2G1 and LiDAR

The T2G1 survey integrated the GPR depth slices of 0.4m – 0.6m, 1.4m – 1.6m and 2.4m – 2.6m with the LiDAR intensity image. The correlation between the LiDAR intensity values and the GPR depth slices is excellent. A change in LiDAR intensity is seen moving across the T2G1 survey area from North (higher intensity) to the south (lower intensity). This difference is mirrored in the underlying sediments, with the 1.4m – 1.6m and 2.1m – 2.6m showing the difference between T2A1 (lower reflecting area) and T2A2 (higher reflecting area). Again the reflectance properties of the GPR depth slices change through the profile, with the depth slice of 0.4m – 0.6m showing a general area of high reflection, not displaying the same variation as the two deeper depth slices. It is again interpreted that the changes in the LiDAR intensity and the GPR reflectance values is caused by a change in the soil moisture content, itself a product of the sedimentary architecture. This again the highlights the potential of using LiDAR intensity values as a means of identifying variation in sediment structure.

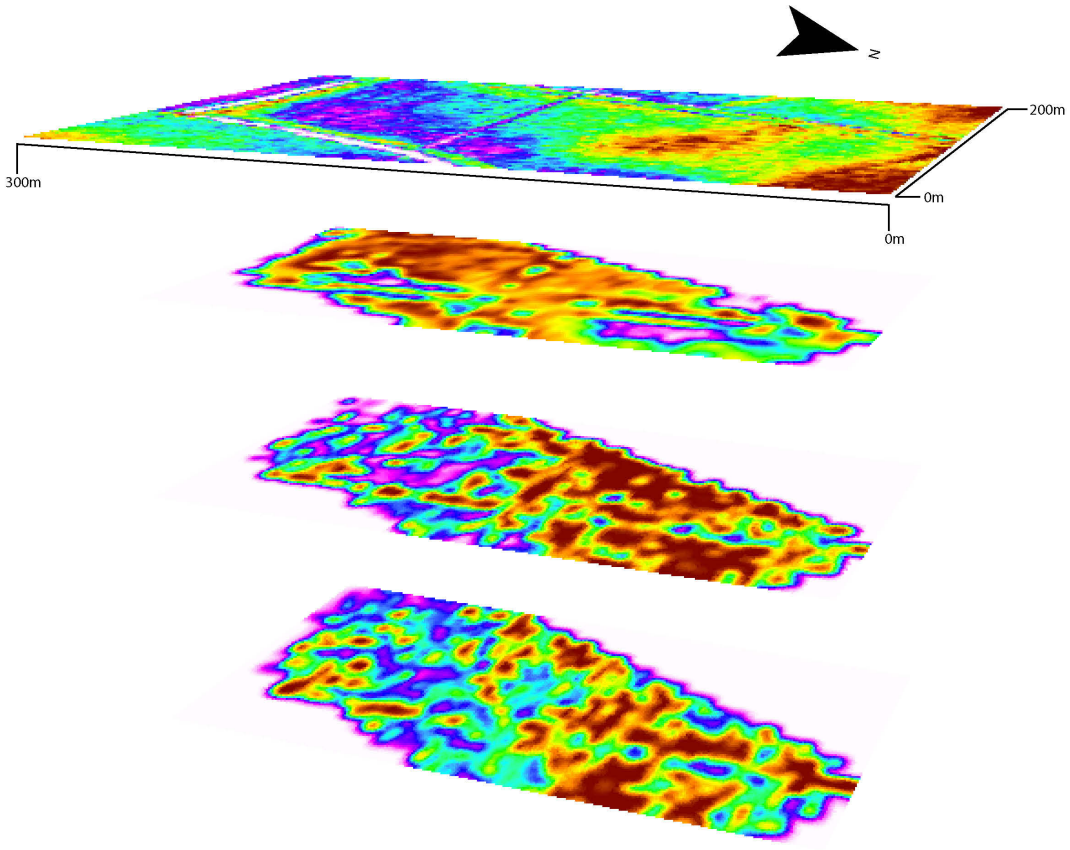

Fig 6.4: The T2G1 survey combining the GPR depth slices of 0.4m – 0.6m, 1.4m – 1.6m and 2.4m – 2.6m with the LiDAR intensity.